Bio-based Rigid Polyurethane Foam Prepared from Apricot Stone Shell-based Polyol for Thermal Insulation Application - Part 2: Morphological, Mechanical, and Thermal Properties

Muhammed Said Fidan * and Murat Ertaş

The procedure for the liquefaction of apricot stone shells was reported in Part 1. Part 2 of this work determines the morphological, mechanical, and thermal properties of the bio-based rigid polyurethane foam composites (RPUFc). In this study, the thermal conductivity, compressive strength, compressive modulus, thermogravimetric analysis, flammability tests (horizontal burning and limited oxygen index (LOI)) in the flame retardants), and scanning electron microscope (SEM) (cell diameter in the SEM) tests of the RPUFc were performed and compared with control samples. The results showed the thermal conductivity (0.0342 to 0.0362 mW/mK), compressive strength (10.5 to 14.9 kPa), compressive modulus (179.9 to 180.3 kPa), decomposition and residue in the thermogravimetric analysis (230 to 491 °C, 15.31 to 21.61%), UL-94 and LOI in the flame retardants (539.5 to 591.1 mm/min, 17.8 to 18.5%), and cell diameter in the SEM (50.6 to 347.5 µm) of RPUFc attained from liquefied biomass. The results were similar to those of foams obtained from industrial RPUFs, and demonstrated that bio-based RPUFc obtained from liquefied apricot stone shells could be used as a reinforcement filler in the preparation of RPUFs, specifically in construction and insulation materials. Moreover, liquefied apricot stone shell products have potential to be fabricated into rigid polyurethane foam composites.

Keywords: Thermal properties; Rigid polyurethane foam; Apricot stone shell; Morphological properties; Characterization

*Contact information: Department of Forest Industry Engineering, Faculty of Forestry, Bursa Technical University, 16310, Bursa, Turkey; *Corresponding author: said.fidan@btu.edu.tr*

INTRODUCTION

The rigid polyurethane foams (RPUFs) industry is still intensely petroleum-dependent because its two major feedstocks, isocyanates and polyols, are petroleum derived. Nevertheless, due to uncertain prices of petroleum in the future, and the need to move towards more environmentally friendly feedstocks, many recent attempts have concentrated on replacing all or part of the conventional petroleum-based polyols by alternatives attained from renewable resources (Gama *et al.* 2015a).

Rigid polyurethane foams are a class of lightweight porous materials of tremendous interest due to their potential application and specific properties in various areas. They can be categorized as rigid, semi-rigid, and flexible foams, relying on the mechanical characteristics, density, and cell morphology. Among the foamed polymers used commercially, RPUFs have the lowest thermal conductivity (Gama *et al.* 2015a).

Various processes that produce non-petroleum derived polyols and many non-petroleum resources are used in polyurethane foam fabrication. Processes include the acid liquefaction of various biomass residuals, and the modification of vegetable oils, such as oxypropylation (Aniceto *et al.* 2012). Additionally, various sequencing strategies are used to fabricate renewable polyols for the polyurethane foam industry (Gama *et al.* 2015a).

The acid liquefaction of biomass resources to fabricate bio-based rigid polyurethane foams can include bamboo (Xie *et al.* 2014), coffee grounds (Gama *et al.* 2015a), cork (Gama *et al.* 2015b; Esteves *et al.* 2017), corn stalk (Yan *et al.* 2008), corn bran (Lee *et al.* 2000), cotton burrs (Fidan and Ertaş 2020a), eucalyptus, pine woods (Ertaş *et al.* 2014), lignin (Xue *et al.* 2015; Mahmood *et al.* 2016), pine bark and peanut shell (Zhang *et al.* 2020), soybean straw (Hu *et al.* 2012), sugar-cane bagasse (Hakim *et al.* 2011; Xie *et al.* 2015), waste paper (Lee *et al.* 2002), wheat straw (Chen and Lu 2009), wood bark (Zhao *et al.* 2012), wood powder (Zhang *et al.* 2013), and yaupon holly (Huang *et al.* 2017a).

The construction industry can play a significant role in sustainable development. The use of environment-friendly materials in modern buildings not only can considerably decrease construction waste, but it also avoids excessive use of natural resources. When considering the industry's position, the utilization of biomass resources, particularly crop residuals, is an effective way to protect the environment and to save energy in the building industry. Utilization of biomass can greatly decrease CO_2 emissions (Zhang *et al.* 2020).

In the construction of buildings, RPUFs are a polymer material widely used for sound absorption and thermal insulation due to their thermal stability (Czuprynski *et al.* 2010; Vitkauskiene *et al.* 2011; Luo *et al.* 2016; Sung *et al.* 2016; Tiuc *et al.* 2016; Zhang *et al.* 2020). They have easy combustion, low density, and a large surface area (Modesti *et al.* 2001; Tang *et al.* 2002; Levchik and Weill 2004; Chen *et al.* 2019). They must be properly modified because of their low fire retardant capacity. As such, the preparation of RPUFs with increased fire resistance has rendered them flame retardant (Czech-Polak *et al*. 2016). In regard to bio-based RPUFs, bio-based polyols, which could be fabricated from plant fibers (Zhang *et al*. 2013; Xie *et al.* 2015; Zhang *et al.* 2020) and vegetable oils (Kuranska and Prociak 2016), are commonly served as raw materials owing to the existence of abundant hydroxyl groups or double bonds in these polyols (Zhang *et al.* 2020).

The raw material used to produce renewable polyols in this study was apricot stone shell. It is an agricultural product of high economic and ecological benefit. The utilization of biomass, especially crop wastes, is an effective way to save energy and protect the environment in the building industry. Therefore, the utilization of biomass resources will substantially decrease excessive CO_2 emissions. The aim of this study was to obtain the following properties of RPUFc: compressive strength, compressive modulus, thermal conductivity, as well as conduct thermogravimetric analysis, flammability tests and scanning electron microscopy analysis.

EXPERIMENTAL

Materials

The apricot stone shells were collected at Kahramanmaras Agricultural Research Institute, Kahramanmaras, Turkey. They were collected in 37°32'08 K, 37°32'08 D and 467 altitude at local plantations.

The procedure for the liquefaction of apricot stone shell was reported in Part 1. In this article, the apricot stone shells, having a particle size of 125 µm, were liquefied with a PEG-400 (polyethylene glycol-400) and glycerin mixture in the presence of sulfuric acid catalyst at 140 to 160 °C for 120 min. The rigid polyurethane-type foam composites from the reaction were successfully prepared with different chemical materials. The results demonstrated that biobased polyurethane-type foam composites were successfully produced from the liquefied apricot stone shell. The FTIR spectra of liquefaction products confirmed the successful liquefaction of products and that they are sources of hydroxyl groups. The liquefaction yield (81.6 to 96.7%), hydroxyl number (133.5 to 204.8 mg KOH per g), the highest elemental analysis amount (C, H, N, S, O) (62.08, 6.32, 6.12, 0.13, and 25.35%), and density (0.0280 to 0.0482 g per cm^3) of the rigid polyurethane foam composites were comparable to foams made from commercial RPUF composites (Fidan and Ertaş 2020b).

In part 2 of this work the morphological, mechanical, and thermal properties of the bio-based rigid polyurethane foam composites (RPUFc) were determined.

Methods

Characterization tests were performed on four types of foam (Foam Code: RPUFc-75, RPUFc-100, RPUFc-125, RPUFc-150) according to the different rate of polymeric diphenylmethane diisocyanate (pMDI 75-100-125-150) and synthetic foam (RPUFc).

Characterization of RPUFc

A BT604 universal mechanical test analyzer (Testform, Bursa, Turkey) was used to measure the compressive properties of the RPUFc. Samples (30 × 30 × 30 mm^3) were placed between the two parallel plates and compressed at 10 mm/min. Six replicates were determined for each group.

The compressive modulus was calculated by the slope of the tangent of the linear part in the stress-strain profile according to the method defined in former studies (Huang *et al.* 2017a). The compressive modulus was determined according to ASTM D1621-10 (2010). The compressive modulus was obtained from the stress-strain curve at a deformation of 10%. Six replicates were determined for each sample.

The thermal conductivity of RPUFc was measured *via* a FOX 314-95ET (Laser Corporation, New Castle, USA). A 10-min read time was used to minimize the contact resistance errors. Thermal conductivity was performed according to ASTMD C518 (2017). Ten replicates were carried out for each group and the average was reported.

The thermogravimetric analyses (TGA/DTG) of all RPUFc and the raw material were determined with a thermal analyzer STA 7200 (Hitachi, Japan) to simultaneously obtain thermogravimetric data. TG/DTG was used to measure the thermal degradation of RPUFc. Specimen weight was between 5 and 10 mg. Each sample was conducted at 30 °C to 800 °C with a constant heating rate of 10 °C/min under a flow rate of 200 mL/min of nitrogen atmosphere.

Horizontal burning (UL-94) tests were conducted *via* the UL-94 test in regard to ASTM D635-14 (2014). The RPUFc was cut into five pieces with dimensions of 125 × 10 × 13 mm^3. The burning rate was determined based on Eq. 1,

$$V = (60 \times L) / t \quad (1)$$

where V is the burning rate (mm/min), L is the burned length (mm), and t is time (s).

The LOI tests were performed using an LOI instrument according to ASTM D2863-97 (2019). Samples were prepared in dimensions of 100 × 10 × 10 mm^3. The LOI measurements for each sample were repeated five times.

Scanning electron microscopy (SEM) (Gemini 300; Carl Zeiss, Oberkochen, Germany) was used to examine the morphology of the RPUFc. Prior to analysis, the specimens were coated in gold using an EM ACE600 (Leica; Carl Zeiss, Oberkochen, Germany). Images of the cross-sections of RPUFc were demonstrated. The mean cell diameter was determined from 50 measurements.

The data gathered as a result of the tests performed were recorded in Microsoft Excel (Version 2016, Redmond, WA, USA). The arithmetic averages, standard deviations, and coefficient of variation were calculated for each test and shown in related charts. Afterwards, the statistical analysis of the obtained findings was conducted. The variance analyses of findings were performed according to the Duncan test by using the SAS statistical program (SAS Institute Inc., Version 6.0, Cary, NC, USA).

The results of compressive strength and modulus samples were used to manage an analysis of variance employing a randomized block factorial experimental design using the SAS statistical program. The mean values were compared using the Duncan test. Ultimately, multiple correlation analysis was performed in an attempt to analyze the relationship between groups.

RESULTS AND DISCUSSION

SEM Analysis

As presented in Fig. 1, the RPUFc based on the pMDI ratio had a comparatively small cell diameter. The cell diameters were measured on the surface of the RPUFc with different pMDI ratios derived from liquefied apricot stone shell. The values are listed in Table 1.

The cell diameters of foams with RPUFc-75, RPUFc-100, RPUFc-125, RPUFc-150, and the control (RPUFc) based on the pMDI ratio were 115.4, 128.4, 131.6, 162.4, and 207.0 μm, respectively (Table 1).

Table 1. Cell Diameters of the RPUFc

Foam Code	Cell Diameter (μm)
RPUFc-75	115.38
RPUFc-100	128.39
RPUFc-125	131.59
RPUFc-150	162.43
RPUFc	207.02

The cell diameters ranged between 50.6 and 238.7 μm in RPUFc-75, between 51.4 and 301.3 μm in RPUFc-100, between 63.4 and 309.2 μm in RPUFc-125, between 67.4 and 316.5 μm in RPUFc-150, and between 77.1 and 347.5 μm in RPUFc. The increase in the pMDI increased the cell diameter. When higher numbers of pMDI were used, the ensuing foams had more cells with larger diameters (Fig. 1).

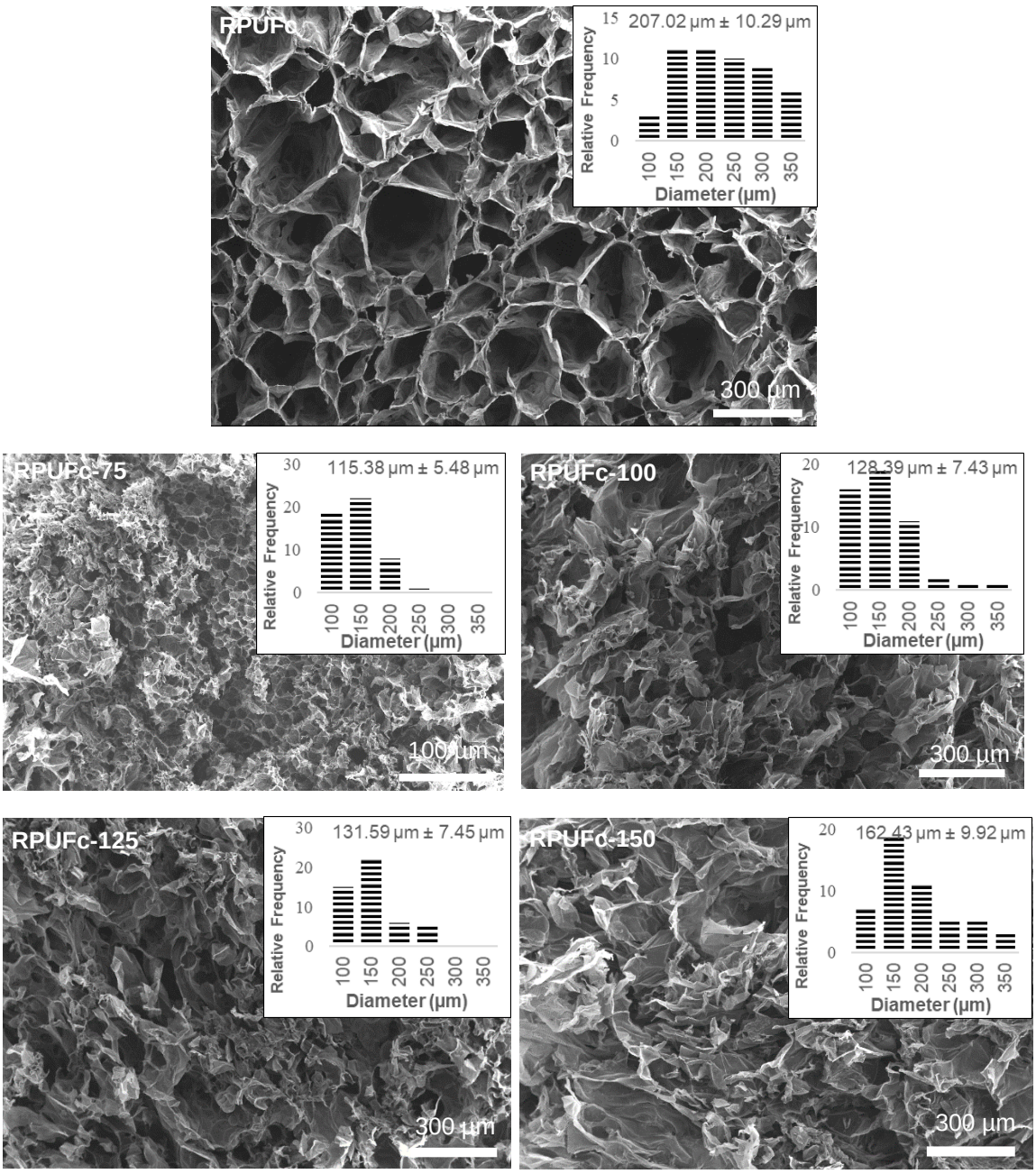

Fig. 1. The SEM images of the RPUFc (Magnification: x30, Accelerating voltage: 15 kv)

As reported in the literature, the cells are usually closed. Because the pore size and cell structure of RPUF are closely connected to their mechanical properties and thermal conductivity, it is necessary to characterize the microstructure of biofoams (Gama *et al.* 2015a). These RPUF had closed cells with a polyhedral structure, differing from the open cellular structure generally observed for flexible polyurethane foams. The use of 100% bio-based polyol for RPUF production afforded foams that were dominated by smaller pore size and greater homogeneity (Esteves *et al.* 2017). Akdogan *et al.* (2019) speculated that small changes in the number of closed cells, similar to those in their own work, did not have an important effect on compressive strength and thermal conductivity. It was found that the foam cells were more regular and smooth with an increased isocyanate index from

105 to 150. At an isocyanate index between 105 and 135, the pore diameter gradually grew from 161.5 µm to 242.1 µm. Conversely, with a further surge in the isocyanate index to 150, pore diameter dropped to 223.5 µm. It is conceivable that the increase of pore diameter contributed to the increased amount of CO_2 that correlated with an increasing isocyanate index. Nevertheless, the diminishing pore size at PU150 was probably due to increasing cell wall elasticity, which could attribute to restricting the CO_2 blowing and expanding, resulting in a smaller pore diameter (Huang *et al.* 2017a).

Compressive Strength and Modulus

The mean values and the groups resulting from the Duncan analysis of the compressive strength and modulus of RPUFc are listed in Table 2. The differences in the compressive strength and modulus were significant to a level of 1% for the effects of RPUFc-75, RPUFc-100, RPUFc-125, RPUFc-150, and RPUFc.

Table 2. Mean Values and Groups Resulting from the Duncan Analysis of the Compressive Strength and Modulus of the RPUFc

Foam Code	Compressive Strength (kPa)	Compressive Modulus (kPa)
RPUFc-75	10.51^{c} *2.87*	179.907^{a} *0.93*
RPUFc-100	11.44^{c} *3.24*	179.986^{a} *0.02*
RPUFc-125	11.71^{bc} *2.33*	180.147^{a} *0.17*
RPUFc-150	14.92^{ab} *0.40*	180.123^{a} *0.09*
RPUFc	15.90^{a} *6.70*	180.260^{a} *0.46*

*Groups with same letters in a column demonstrate that there is no statistical difference ($P < 0.05$) between the samples in regard to Duncan's multiply range test; **the values in italics are standard deviation

As shown in Table 2, by increasing the polymeric diphenylmethane diisocyanate (pMDI) content from 75% to 150%, the compressive strength increased from 10.5 to 14.9 kPa, and the compressive modulus ranged from 179.9 to 180.3 kPa, respectively. The impact of the pMDI amount on mechanical properties of the RPUFc was similar to that on density. The amount of compressive strengths and modulus of RPUFc-75, RPUFc-100, RPUFc-125, and RPUFc-150 was lower than commercial foams.

The range of compression stress at 10% deformation values reported for the PUFs obtained from liquefied cork was determined. It ranged from 7.7 to 34.6 kPa, and the modulus of elasticity (MOE) ranged from 183 to 475 kPa (Gama *et al.* 2015a). Furthermore, the PUFs obtained from liquefied corn bran were reported to have a compressive strength at 10% strain of 76 kPa, and a compressive MOE of 140 kPa (Lee *et al.* 2000; Esteves *et al.* 2017). The compressive strength and modulus of RPUFc produced in this work was similar to those of liquefied cork and corn bran-derived PU foam.

Moreover, due to the increase of the extent of bagasse liquefaction, the morphological features of the residue had a higher surface area and were more homogeneous. This resulted in much better adhesion between the bagasse residual and polyurethane (PU). Thus, better the compressive strength (CS) could be obtained. Additionally, it should be noted that at a fixed rate of isocyanate with the amount of weight

percentage of bagasse residue, unreacted ingredients during liquefaction could not ensure influential strength of the RPUFc. The higher the bagasse residual amount, however poor the mechanical properties, the lower the economic price for the RPUFc. Hence, the balance point between the mechanical properties and economic price should be reached using a practical application (Xie *et al.* 2015).

Thermal Conductivity

Thermal conductivity of RPUF is a parameter that is fundamental to indicating thermal insulation properties. This characteristic of an RPUF depends on various factors, such as the mean density, cell size, cell orientation, thermal conductivity of the blowing agent in the cells, and closed-cell content of RPUF. As shown in Fig. 2, the thermal conductivity value of RPUFc was found to vary from 0.0342 to 0.0362 mW/mK, with the growth of pMDI from 75 to 150, and the minimum value (0.0342 mW/mK) was obtained from RPUFc-150. It was demonstrated that the thermal conductivity values of the RPUFc made with RPUF-125 and RPUFc-150 were lower than that of RPUFc, contrary to RPUF-75 and RPUFc-100. It was clearly apparent that the presence of pMDI in the foam matrix caused an increase in the thermal conductivity and mean cell size values.

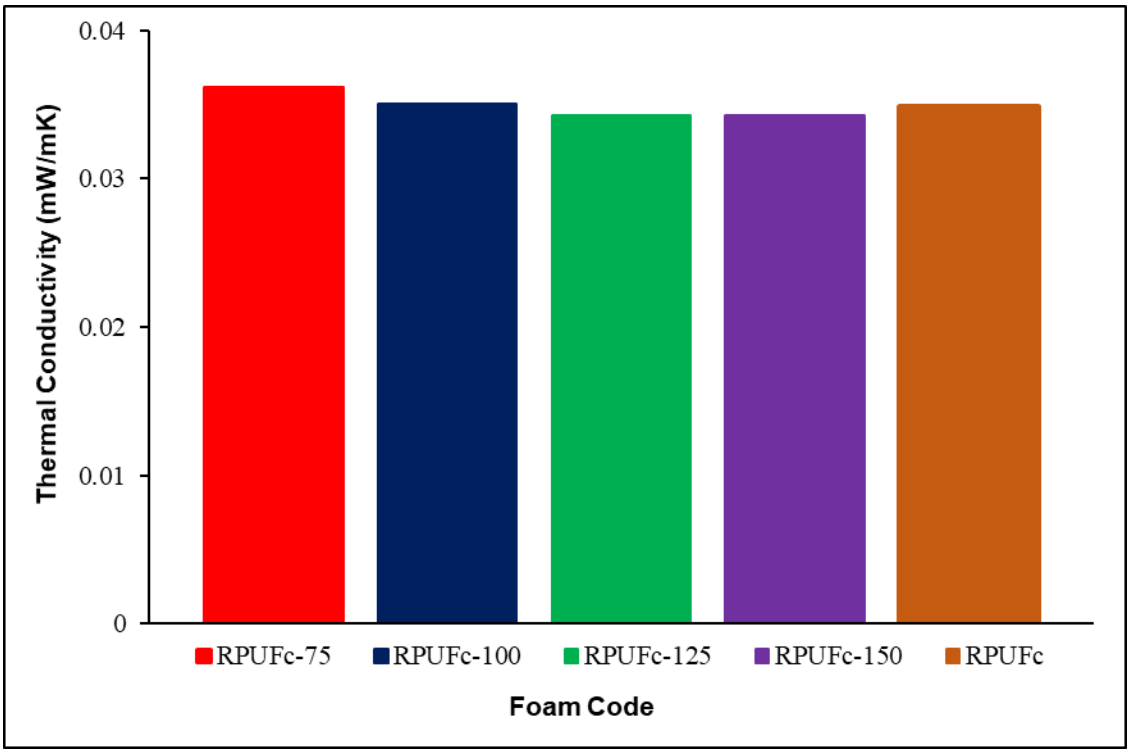

Fig. 2. The thermal conductivity of the RPUFc

It was demonstrated that the thermal conductivity value of biofoams gradually increased from 0.035 to 0.037 mW/mK simultaneously with an increasing isocyanate index from 105 to 135 (Huang *et al.* 2017a). It should be noted that biofoams were satisfactory for use as insulation foam with thermal conductivity values between 0.0233 and 0.0505 mW/mK (Gama *et al.* 2015a; Mahmood *et al.* 2016). The thermal conductivity numbers were akin to those of corn-stover-derived foam ranging from 0.032 to 0.039 mW/mK (Hu and Li 2014).

The results were ascribed to the variation of foam density. Generally, thermal conductivity is conversely proportional to the density of the PU foam, presumably due to the lower radiant heat transfer ratio through the gases trapped in small cells (Huang *et al.* 2017a). Thermal conductivity is the key thermal property that governs insulation applications of RPUFc. It is closely associated with cell morphology (the rate that closed cells open), cell orientation, and foam density (Huang *et al.* 2017a). There is a powerful relation between the thermal conductivity and mean cell diameter, namely, the smaller the mean cell diameter, the greater reduction in the thermal conductivity (Akdogan *et al.* 2019).

Low thermal conductivity derives from high closed-cell contents and small average cell size (Mahmood *et al.* 2016). The low thermal conductivity values attained for the coffee grounds derived RPUFs make them good candidates for use in thermal insulation equipment with potential applications in upholstery, refrigerator trucks, and buildings (Gama *et al.* 2015a).

Thermogravimetric Analysis

Figures 3 and 4 show the thermal degradation behaviors (TGA and DTG) of the RPUFc from liquefied apricot stone shell under nitrogen atmosphere. Also, Table 3 summarizes the thermal degradation of the of RPUFc from liquefied apricot stone shell under nitrogen environment.

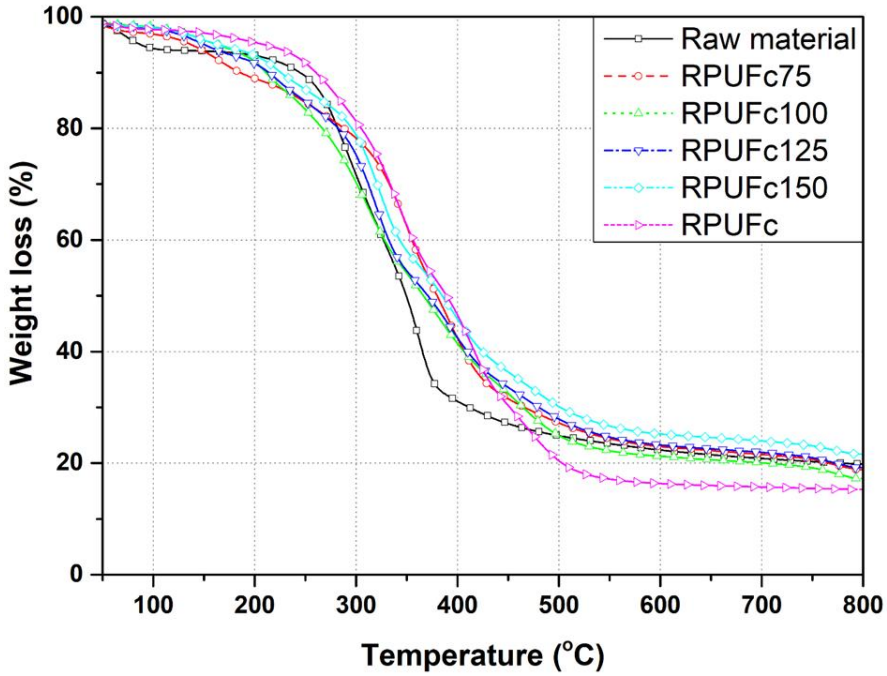

Fig. 3. The TGA curve of the RPUFc under nitrogen atmospehere

The T_{onset} refers to the degradation temperature at 5% the weight loss, and T_{max} also corresponds to temperature of maximum rate of degradation.

As shown in Figures 3 and 4, all RPUFc from liquefied apricot stone showed similar TGA and DTG curves and shapes, suggesting smilar thermal degradation behaviours. The weight loss up to about 165 °C was considered to result from the release of thermally unstable diethylene glycol and the evaporation of the moisture content (Table 3). The onset

degradation temperatures (T_{onset}) of the RPUFc from liquefied apricot stone was in the range of 230.0 °C to 282.6 °C, which was slightly than higher that of the synthetic foam. Moreover, the onset degradation and the maximum degradation tempratures of the RPUFc-75 was higher than those of the synthetic foam and other biofoams, which attributed to the substitution of petroleum-based polyol with bio-based polyol from liquefaction. This improved the thermal stability of rigid PU foam due to the enhancement of the urethane linkage density of the bio-based polyol with multi hydroxyl groups (C5 and C5 sugars) (Huang *et al.* 2018). On the other hand, the thermal stability of the RPUFc from liquefied apricot stone slightly decreased with the increase of the pMDI (polymeric methylene diphenyl diisocyanete) rate because of the presence of thermally unstable pMDI.

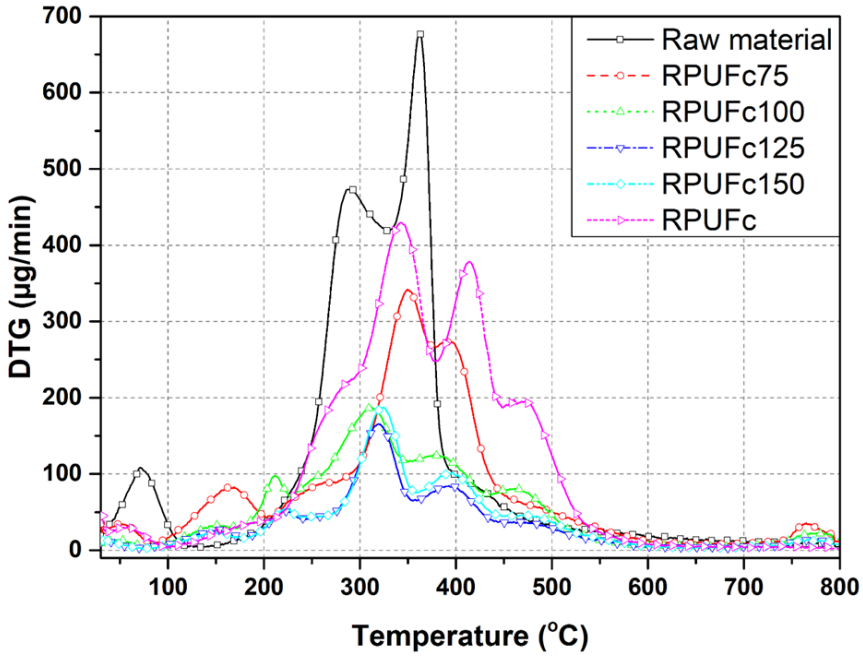

Fig. 4. The DTG curve of the RPUFc under nitrogen atmosphere

The first degradation stage between 312 °C and 349 °C, could be attributed to the unstable urethane groups and partially to the degradation of diethylene glycol (Hablot *et al.* 2008; Huang *et al.* 2017a; Akdogan *et al.* 2019). The second stage of the important weight loss was at roughly 390 °C, which could be assigned to the degradations of polyol and liquefied wood components (Zhao *et al.* 2012; Hu and Li 2014; Huang *et al.* 2017a; Janković *et al.* 2019; Šoštarić *et al.* 2020). Furthermore, due to the presence of liquefied waste in the samples, the degradation of bagasse constitutions (*i.e.*, cellulose and hemicellulose) occurred in this temperature range (Xie *et al.* 2015). Eventually, the third stage centered at nearly 480 °C was ascribed to the degradation of lignin and other more sturdy compenents (Huang *et al.* 2017a; Ertaş *et al.* 2014). Furthermore, this stage also corresponded to the degradation of pMDI. The thermal degradation and stability behavior of all RPUFc from liquefied apricot stone shells were similar to those of sugarcane bagasse, yaupon holly, apricot kernel shells and apricot shells-derived PU foam (Xie *et al.* 2015; Huang *et al.* 2017a; Janković *et al.* 2019; Šoštarić *et al.* 2020).

Table 3. TGA and DTG Data of the Raw Material and the RPUFc Under Nitrogen Atmosphere

Foam Code	T_{onset} (°C)	T_{max} (°C)			Residue at 800 °C (%)
		Stage 1	Stage 2	Stage 3	
Raw material	273.3	362.4	420.3	-	19.85
RPUFc-75	282.6	349.2	399.1	491.0	18.86
RPUFc-100	230.0	312.1	377.9	459.9	17.23
RPUFc-125	257.6	319.2	391.9	476.7	19.22
RPUFc-150	263.7	324.6	393.6	477.6	21.61
RPUFc	267.7	342.3	396.5	470.5	15.31

T_{onset}: temperature at 5% the weight loss; T_{max}: temperature of maximum rate of degradation.

The residue yields of the RPUFc from liquefied apricot stone were higher than that of the synthetic foam, which was due to the cross-linkage cellular structure and the introduction of ash components from apricot stone (Huang *et al.* 2017b). Similar tendency has been reported in the literature (Ertaş *et al.* 2014; Huang *et al.* 2018).

Flammability Tests (UL-94 and LOI)

Figure 5 shows the effect of the RPUFc on the ratio of flame retardants using the vertical burning test (UL-94) and LOI.

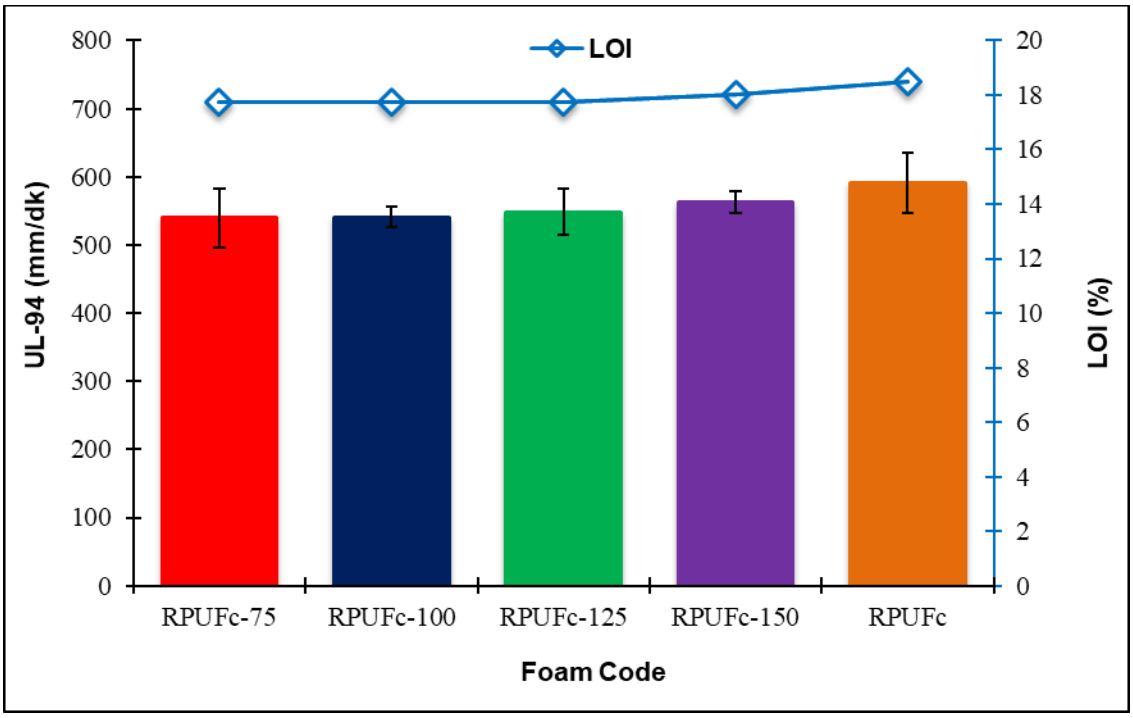

Fig. 5. The UL-94 and LOI properties of the RPUFc

As shown in Fig. 5, the flame spread rate demonstrated a rise with the increase in the amount of pMDI. The values UL-94 V were determined for pMDI-75, pMDI-100, pMDI-125, pMDI-150, and the control (RPUFc), which respectively increased to 539.5, 540.9, 548.3, 562.3, and 591.1 mm/min. The foams of RPUFc-75, RPUFc-100, RPUFc-

125, RPUFc-150, and the control (RPUFc) did not catch fire owing to the higher loading level of fire resistance. This statement was also confirmed by the results obtained during the UL-94 V test.

The LOI is a measure of the percent of oxygen. Air involves roughly 21% oxygen, and, hence, any equipment with a LOI value of less than 21% will presumably support burning in open air (Akdogan *et al.* 2019). As a result, the lower the flammability value, the higher the LOI. While the LOI of RPUFc was determined as 18.5%, this value for RPUFc-75, RPUFc-100, RPUFc-125, and RPUFc-150 rose to 17.8, 17.8, 17.8, and 18%, respectively. At the same time, there were no significant differences at the time the flame went out (Czech-Polak *et al.* 2016).

The addition of flame retardants to RPUF shifted the apparent density only relatively, but had important effects on the fire resistance. The values of LOI for prepared compositions containing flame retardants were higher than 28%, allowing them to qualify as flame resistant materials (Czech-Polak *et al*. 2016).

CONCLUSIONS

1. The SEM micrographs of RPUFc with different levels of pMDI demonstrated that the cellular structure depends on the characteristics of the polyol used.
2. The compressive strength, and compressive modulus of the resulting RPUFc were 14.9 kPa, and 180.1 kPa, respectively. In the mechanical properties, the RPUFc obtained with increased pMDI content was decreased as compared to control samples. In the mechanical properties, the RPUFc obtained with increased pMDI content was decreased as compared to control samples. The compressive strength and modulus values of almost all the obtained composites were lower than that of the RPUF.
3. The thermal conductivity of the resulting RPUFc was 0.0342 mW/mK. The thermal conductivities of the obtained rigid polyurethane foam composites were lower than that of the RPUF.
4. The thermal stability of the RPUFc-75 was greater than that of synthetic foam, indicating that the substitution of petroleum-based polyol with liquefaction bio-based polyol had a positive influence on the thermal stability of rigid PU foams. However, the thermal stability of the RPUFc from liquefied apricot stone slightly decreased with the increase of the pMDI loading. The thermal conductivity and thermal stability of the RPUFc obtained were within the values registered for other RPUFs derived from renewable resources, making them suitable for thermal insulation.
5. The values for UL-94 and LOI low-density RPUFc were 562.3 mm/min and 17.8%, respectively. Moreover, the cell diameter of the resulting low-density RPUFc-150 was 162.4 μm. The flame spread rates for RPUFc obtained with an increase in the pMDI ratio described a reduction in comparison with the RPUFs.
6. The morphological, mechanical, and thermal property characterization results demonstrate that the foam properties depended on the percentage of the physical blowing agent and the percentage of bio-contents of the apricot stone shell-based polyols.

7. When considering the industry's position, the utilization of biomass resources, especially crop residuals, is an effective way to protect the environment and to conserve energy in the building industry. The utilization of biomass will significantly reduce CO_2 emissions. Various processes that produce non-petroleum derived polyols and many non-petroleum resources are used in polyurethane foam production. For these reasons, as a consequence of the present study, the RPUFc-150 obtained from liquefied apricot stone shells could be used as a reinforcement filler in the preparation of RPUFc. It is noteworthy that this RPUFc could be used as construction and insulation material.

ACKNOWLEDGEMENTS

The authors thank the Department of Forest Industry Engineering Laboratory and Central Research Laboratory at the University of Bursa Technical University, Bursa, Turkey.

REFERENCES CITED

Akdogan, E., Erdem, M., Üreyen, M. E., and Kaya, M. (2019). "Rigid polyurethane foams with halogen-free flame retardants: Thermal insulation, mechanical, and flame retardant properties," *Journal of Applied Polymer Science* 137(1), Article ID 47611. DOI: 10.1002/app.47611

Aniceto, J. P. S., Portugal, I., and Silva, C. M. (2012). "Biomass-based polyols through oxypropylation reaction," *ChemSusChem* 5(8), 1358-1368. DOI: 10.1002/cssc.201200032

ASTMD C518 (2017). "Standard test method for steady-state thermal transmission properties by means of the heat flow meter apparatus," ASTM International, West Conshohocken, PA, USA.

ASTM D635-14 (2014). "Standard test method for rate of burning and/or extent and time of burning of plastics in a horizontal position," ASTM International, West Conshohocken, PA, USA.

ASTM D1621-10 (2010). "Standard test method for compressive properties of rigid cellular plastics," ASTM International, West Conshohocken, PA, USA.

ASTM D2863-97 (2019). "Standard test method for measuring the minimum oxygen concentration to support candle-like combustion of plastics (oxygen index)," ASTM International, West Conshohocken, PA, USA.

Chen, F., and Lu, Z. (2009). "Liquefaction of wheat straw and preparation of rigid polyurethane foam from the liquefaction products," *Journal of Applied Polymer Science* 111(1), 508-516. DOI: 10.1002/app.29107

Chen, X., Li, J., and Gao, M. (2019). "Thermal degradation and flame retardant mechanism of the rigid polyurethane foam including functionalized graphene oxide," *Polymers* 11(1), Article number 78. DOI: 10.3390/polym11010078

Czech-Polak, J., Przybyszewski, B., Heneczkowski, M., Czulak, A., and Gude, M. (2016). "Effect of environmentally-friendly flame retardants on fire resistance and mechanical properties of rigid polyurethane foams," *Polimery* 61(2), 113-116. DOI: 10.14314/polimery.2016.113

Czuprynski, B., Paciorek-Sadowska, J., and Liszkowska, J. (2010). "Properties of rigid polyurethane-polyisocyanurate foams modified with the selected fillers," *Journal of Applied Polymer Science* 115(4), 2460-2469. DOI: 10.1002/app.30937

Ertaş, M., Fidan, M. S., and Alma, M. H. (2014). "Preparation and characterization of biodegradable rigid polyurethane foams from the liquefied eucalyptus and pine woods," *Wood Research* 59(1), 97-108.

Esteves, B., Dulyanska, Y., Costa, C., Vicente, J., Domingos, I., Pereira, H., De Lemos, L. T., and Cruz-Lopes, L. (2017). "Cork liquefaction for polyurethane foam production," *BioResources* 12(2), 2339-2353. DOI: 10.15376/biores.12.2.2339-2353

Fidan, M. S. and Ertaş, M. (2020a). "Optimization of liquefaction parameters of cotton burrs (*Gossypium hirsutum* L.) for polyurethane-type ısolation foams," *Kastamonu University Journal of Forestry Faculty* 20(1), 15-24.

Fidan, M. S. and Ertaş, M. (2020b). "Biobased rigid polyurethane foam prepared from apricot stone shell based polyol for a thermal insulation application, Part 1: Synthesis, chemical, and physical properties," *BioResources* 15(3), 6061-6079. DOI: 10.15376/biores.15.3.6061-6079

Gama, N. V., Soares, B., Freire, C. S. R., Silva, R., Neto, C. P., Barros-Timmons, A., and Ferreira, A. (2015a). "Bio-based polyurethane foams toward applications beyond thermal insulation," *Materials & Design* 76, 77-85. DOI: 10.1016/j.matdes.2015.03.032

Gama, N., Soares, B., Freire, C. S. R., Silva, R., Brandão, I., Neto, C. P., Barros-Timmons, A., and Ferreira, A. (2015b). "Rigid polyurethane foams derived from cork liquefied at atmospheric pressure," *Polymer International* 64(2), 250-257. DOI: 10.1002/pi.4783

Hablot, E., Zheng, D., Bouquey, M., and Avérous, L. (2008). "Polyurethanes based on castor oil: Kinetics, chemical, mechanical and thermal properties," *Macromolecular Materials and Engineering* 293(11), 922-929. DOI: 10.1002/mame.200800185

Hakim, A. A. A., Nassar, M., Emam, A., and Sultan, M. (2011). "Preparation and characterization of rigid polyurethane foam prepared from sugar-cane bagasse polyol," *Material Chemistry and Physics* 129(1-2), 301-307. DOI: 10.1016/j.matchemphys.2011.04.008

Hu, S., and Li, Y. (2014). "Two-step sequential liquefaction of lignocellulosic biomass by crude glycerol for the production of polyols and polyurethane foams," *Bioresource Technology* 161, 410-415. DOI: 10.1016/j.biortech.2014.03.072

Hu, S., Wan, C., and Li, Y. (2012). "Production and characterization of biopolyols and polyurethane foams from crude glycerol based liquefaction of soybean straw," *Bioresource Technology* 103(1), 227-233. DOI: 10.1016/j.biortech.2011.09.125

Huang, X. Y., Qi, J. Q., De Hoop, C. F., Xie, J. L., and Chen, Y. Z. (2017a). "Biobased polyurethane foam insulation from microwave liquefaction of woody underbrush," *BioResources* 12(4), 8160-8179. DOI: 10.15376/biores.12.4.8160-8179

Huang, X., De Hoop, C. F., Xie, J., Hse, C. Y., Qi, J., and Hu, T. (2017b). "Characterization of biobased polyurethane foams employing lignin fractionated from microwave liquefied switchgrass," *International Journal of Polymer Science* 1, Article ID 4207367. DOI: 10.1155/2017/4207367

Huang, X. Y., De Hoop, C. F., Peng, X. P., Xie, J. L., Qi, J. Q., Jiang, Y. Z., Xiao, H. and Nie, S. X. (2018). "Thermal stability analysis of polyurethane foams made from

microwave liquefaction bio-polyols with and without solid residue," *BioResources* 13(2), 3346-3361. DOI: 10.15376/biores.13.2.3346-3361

Janković, B., Manić, N., Dodevski, V., Radović, I., Pijović, M., Katnić, Đ., and Tasić, G. (2019). "Physico-chemical characterization of carbonized apricot kernel shell as precursor for activated carbon preparation in clean technology utilization," *Journal of Cleaner Production* 236, 117614. DOI: 10.1016/j.jclepro.2019.117614

Kuranska, M., and Prociak, A. (2016). "The influence of rapeseed oil-based polyols on the foaming process of rigid polyurethane foams," *Industrial Crops and Products* 89, 182-187. DOI: 10.1016/j.indcrop.2016.05.016

Lee, S. H., Teramoto, Y., and Shiraishi, N. (2002). "Biodegradable polyurethane foam from liquefied waste paper and its thermal stability, biodegradability, and genotoxicity," *Journal of Applied Polymer Science* 83(7), 1482-1489. DOI: 10.1002/app.10039

Lee, S. H., Yoshioka, M., and Shiraishi, N. (2000). "Liquefaction of corn bran (CB) in the presence of alcohols and preparation of polyurethane foam from its liquefied polyol," *Journal of Applied Polymer Science* 78(2), 319-325. DOI: 10.1002/1097-4628(20001010)78:2<319::AID-APP120>3.0.CO;2-Z

Levchik, S. V., and Weil, E. D. (2004). "Thermal decomposition, combustion and fire-retardancy of polyurethanes—A review of the recent literatüre," *Polymer International* 53, 1585-1610. DOI: 10.1002/pi.1314

Luo, F., Wu, K., and Lu, M. (2016). "Enhanced thermal stability and flame retardancy of polyurethane foam composites with polybenzoxazine modified ammonium polyphosphates," *RSC Advances* 6, 13418-13425. DOI: 10.1039/C5RA27256D

Mahmood, N., Yuan, Z., Schmidt, J., Tymchyshyna, M., and Xu, C. (2016). "Hydrolytic liquefaction of hydrolysis lignin for the preparation of bio-based rigid polyurethane foam," *Green Chemistry* 18, 2385-2398. DOI: 10.1039/C5GC02876K

Modesti, M., Lorenzetti, A., Simioni, F., and Checchin, M. (2001). "Influence of different flame retardants on fire behaviour of modified PIR/PUR polymers," *Polymer Degradation and Stability* 74(3), 475-479. DOI: 10.1016/S0141-3910(01)00171-9

Šoštarić, T., Petrović, M., Stojanović, J., Marković, M., Avdalović, J., Hosseini-Bandegharaei, A., and Lopičić, Z. (2020). "Structural changes of waste biomass induced by alkaline treatment: the effect on crystallinity and thermal properties," *Biomass Conversion and Biorefinery*. DOI: 10.1007/s13399-020-00766-2

Sung, G., Kim, J. W., and Kim, J. H. (2016). "Fabrication of polyurethane composite foams with magnesium hydroxide filler for improved sound absorption," *Journal of Industrial and Engineering Chemistry* 44, 99-104. DOI: 10.1016/j.jiec.2016.08.014

Tang, Z., Maroto-Valer, M. M., Andresen, J. M., Miller, J. W., Listemann, M. L., McDaniel, P. L., Morita, D. K., and Furlan, W. R. (2002). "Thermal degradation behavior of rigid polyurethane foams prepared with different fire retardant concentrations and blowing agents," *Polymer* 43(24), 6471-6479. DOI: 10.1016/S0032-3861(02)00602-X

Tiuc, A. E., Vermeşan, H., Gabor, T., and Vasile, O. (2016). "Improved sound absorption properties of polyurethane foam mixed with textile waste," *Energy Procedia* 85, 559-565. DOI: 10.1016/j.egypro.2015.12.245

Vitkauskiene, I., Makuška, R., Stirna, U., and Cabulis, U. (2011). "Thermal properties of polyurethane-polyisocyanurate foams based on poly(ethylene terephthalate) waste," *Materials Science* 17(3), 249-253. DOI: 10.5755/j01.ms.17.3.588

Xie, J., Qi, J., Hse, C. Y., and Shupe, T. F. (2014). "Effect of lignin derivatives in the bio-polyols from microwave liquefied bamboo on the properties of polyurethane foams," *BioResources* 9(1), 578-588. DOI: 10.15376/biores.9.1.578-588

Xie, J., Zhai, X., Hse, C. Y., Shupe, T. F., and Pan, H. (2015). "Polyols from microwave liquefied bagasse and its application to rigid polyurethane foam," *Materials* 8(12), 8496-8509. DOI: 10.3390/ma8125472

Xue, B. L., Wen, J. L., and Sun, R. C. (2015). "Producing lignin-based polyols through microwave-assisted liquefaction for rigid polyurethane foam production," *Materials* 8(2), 586-599. DOI: 10.3390/ma8020586

Yan, Y., Pang, H., Yang, X., Zhang, R., and Liao, B. (2008). "Preparation and characterization of water blown polyurethane foams from liquefied cornstalk polyol," *Journal of Applied Polymer Science* 110(2), 1099-1111. DOI: 10.1002/app.28692

Zhang, G., Wu, Y., Chen, W., Han, D., Lin, X., Xu, G., and Zhang, Q. (2019). "Open-cell rigid polyurethane foams from peanut shell-derived polyols prepared under different post-processing conditions," *Polymers* 11(9), E1392. DOI: 10.3390/polym11091392

Zhang, G., Zhang, Q., Wu, Y., Zhang, H., Cao, J., and Han, D. (2017). "Effect of auxiliary blowing agents on properties of rigid polyurethane foams based on liquefied products from peanut shell," *Journal of Applied Polymer Science* 134(48), Article ID 45582. DOI: 10.1002/app.45582

Zhang, H., Pang, H., Zhang, L., Chen, X., and Liao, B. (2013). "Biodegradability of polyurethane foam from liquefied wood based polyols," *Journal of Polymers and the Environment* 21, 329-334. DOI: 10.1007/s10924-012-0542-2

Zhang, Q., Lin, X., Chen, W., Zhang, H., and Han, D. (2020). "Modification of rigid polyurethane foams with the addition of nano-SiO_2 or lignocellulosic biomass," *Polymers* 12(1), E107. DOI: 10.3390/polym12010107

Zhao, Y., Yan, N., and Feng, M. (2012). "Polyurethane foams derived from liquefied mountain pine beetle-infested barks," *Journal of Applied Polymer Science* 123(5), 2849-2858. DOI: 10.1002/app.34806

Article submitted: March 24, 2020; Peer review completed: May 31, 2020; Revised version received and accepted: June 12, 2020; Published: June 18, 2020.
DOI: 10.15376/biores.15.3.6080-6094